

A Synthetic Approach to Asymmetric Phthalocyanines with Peripheral Metal-Binding Sites

Marco Haas,^[a] Shi-Xia Liu,^{*[a]} Antonia Neels,^[b] and Silvio Decurtins^[a]

Keywords: N ligands / Asymmetric phthalocyanines / Solid-state structures / Synthesis / UV/Vis spectroscopy

A phthalonitrile derivative **1**, functionalized with two pyridyl groups, undergoes a cyclotetramerization reaction to afford the symmetric metal-free phthalocyanine **2** with peripheral metal-binding sites. In view of its insufficient solubility in organic solvents, a synthetic route to asymmetric peripherally octasubstituted Pcs, which contain a combination of 2,3-di(2-pyridyl)pyrazino and *p*-pentylphenoxy or *p*-(*tert*-butyl)phenoxy substituent groups, has been developed. The compounds

5–9 were synthesized by a statistical condensation reaction between two different phthalonitriles, and remarkably, all of them have been isolated and characterized as single compounds. For structural characterization, an X-ray study of the asymmetric Zn phthalocyanine **11** is given.

(© Wiley-VCH Verlag GmbH & Co. KGaA, 69451 Weinheim, Germany, 2006)

Introduction

The use of phthalocyanines (Pcs) in functional molecular assemblies is widespread.^[1,2] Pcs, also considered synthetic porphyrin analogues, emerge as attractive molecular building blocks due to a variety of characteristic properties. On the one hand, the electronic structure of the Pc^{2-} macrocycle represents a two-dimensional 18 π -electron system, which gives rise to an intrinsic redox activity as well as to intense π - π^* transitions in the visible region. The intense absorption in the red/near-infrared spectral region which, interestingly, contrasts with the absorption behavior of porphyrin analogues, makes Pcs attractive for incorporation into donor-acceptor ensembles, where they function as antennas.^[1,2] On the other hand, Pcs exhibit an architectural flexibility that is well exemplified by a large number of metallic complexes and, importantly, a large variety of substituents can be attached to the macrocyclic core. Moreover, they offer additional advantages such as thermal and chemical stability.

Pcs have been incorporated into a number of molecular and supramolecular systems including porphyrins,^[3] tetra-thiafulvalenes,^[4,5] crown ethers,^[5] and fullerenes,^[6] which all show a variety of potential applications in materials science. However, only a few examples of Pcs and their derivatives with appended ligating groups for metal ions have been reported so far,^[7] mainly due to synthetic difficulties. Nevertheless, they are gaining more interest, and some significant achievements have been reported. For instance, it has been

demonstrated that the direct linking of a terpyridine ligand to ZnPc enables specific sensing for metal ions by monitoring the fluorescence of ZnPc as a function of the added metal ions.^[7a] Another recent investigation has been focused on the study of intramolecular electronic interactions between covalently linked ZnPc and $[\text{Ru}^{\text{II}}(\text{bpy})_3]^{2+}$ units with a variety of spacers.^[7b] It is also worth noting that ZnPcs, bearing two pyridyl substituents at the periphery of the rigid Pc core, self-assemble edge-to-face to form a zig-zag polymer in the solid state,^[7c] although in general, Pcs show a strong propensity to form cofacial or nearly cofacial molecular assemblies.

Our interest in the use of peripherally functionalized Pcs^[7,8] as ligands to form supramolecular systems with multiple functions has also led us to investigate the synthesis of asymmetric peripherally substituted Pcs. Thereby, 2,3-di(2-pyridyl)-6,7-dicyanoquinoxaline has been chosen as one key precursor. Molecules of the 2,3-di(2-pyridyl)quinoxaline type possess conformational flexibility, and thus, offer both monodentate and chelating coordination sites. These structural features have been evidenced by X-ray analysis, which shows that such types of diimine ligands bind metal ions either by N atoms of the pyridine and the pyrazine rings, forming five-membered rings, or only through N atoms of the pyridine rings disposed in a *cis* conformation, forming seven-membered rings.^[9] Consequently, these ligands have been used for the construction of elaborate metal complexes, which show interesting spectroscopic and redox properties as well as intercalation interactions with DNA duplexes.^[10]

In this paper, we report on the synthesis and characterization of i) a symmetric octasubstituted metal-free Pc (H_2Pc) bearing eight pyridyl groups and ii) asymmetric peripherally octasubstituted H_2Pcs and a ZnPc, which contain

[a] Departement für Chemie und Biochemie, Universität Bern, Freiestrasse 3, 3012 Bern, Switzerland
Fax: +41-31-631-3995
E-mail: liu@iac.unibe.ch

[b] Institut de Microtechnique, Université de Neuchâtel, Rue Emile Argand 11, 2009 Neuchâtel, Switzerland

a combination of 2,3-di(2-pyridyl)pyrazino and *p*-pentylphenoxy or *p*-(*tert*-butyl)phenoxy substituent groups. Taking into account that exploitation of Pcs in materials science demands good solubility and low aggregation, we note that the *p*-pentylphenoxy and bulky *p*-(*tert*-butyl)phenoxy groups provide these latter compounds with sufficient solubility in organic solvents for that purpose. These asymmetric Pc compounds were synthesized by a statistical condensation reaction between two different phthalonitriles, and the mixed products were finally separated and isolated by chromatographic techniques.

Results and Discussion

Synthesis of a Symmetrical Octasubstituted H₂Pc (2)

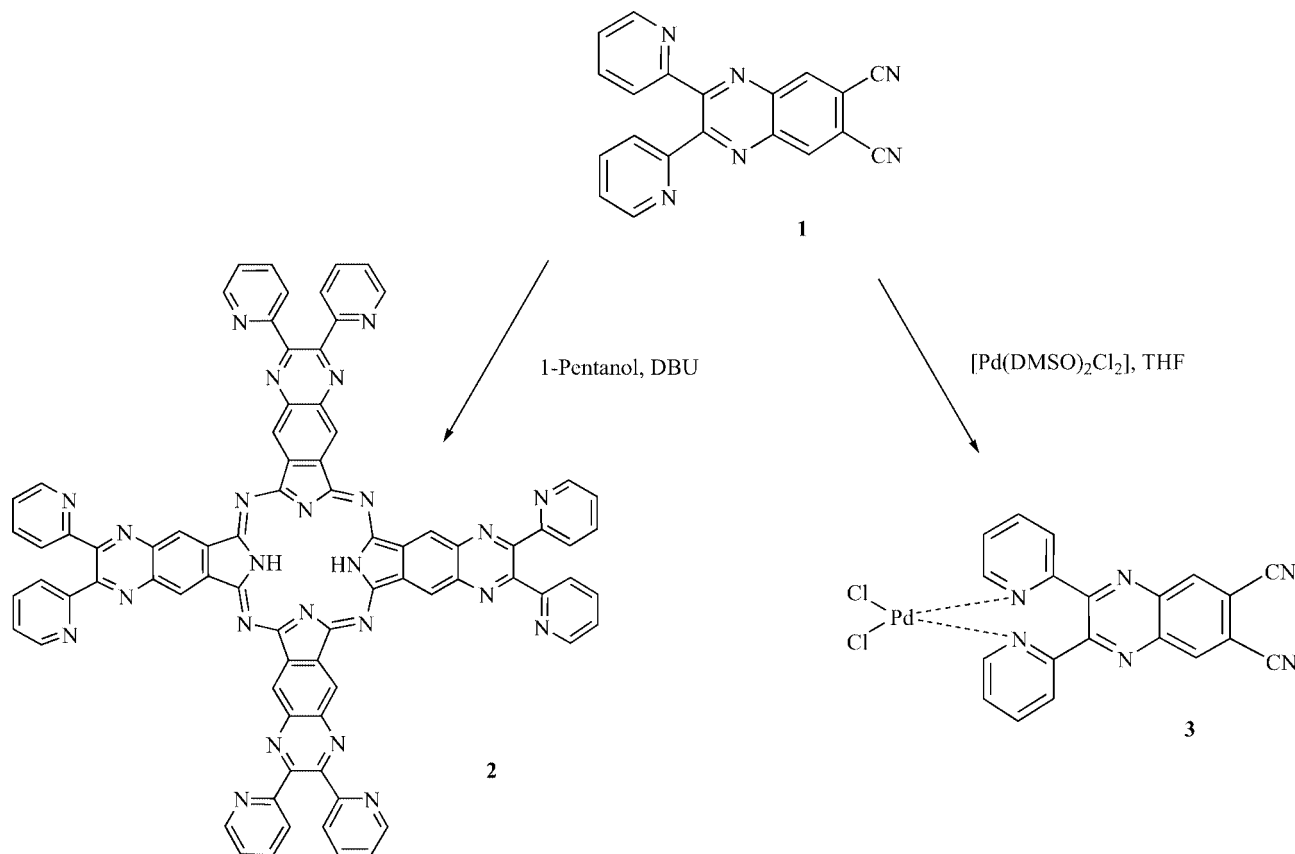
Previously, we reported a synthetic route to a symmetric, fully conjugated, phenanthroline-appended Pc.^[8] However, we observed that this planar extended Pc system exhibits a high degree of insolubility in common organic solvents. As a continuation of that work, Pc **2** (see Scheme 1), bearing eight conformationally flexible pyridyl groups at the periphery, has now been obtained by a direct cyclotetramerization of 2,3-di(2-pyridyl)-6,7-dicyanoquinoxaline (**1**) in the presence of lithium pentoxide at 100 °C under N₂, followed by treatment with glacial acetic acid (Scheme 1). The phthalonitrile derivative **1** was obtained via a Schiff's base condensation of 2,2'-pyridil and 4,5-diaminophthalonitrile;

the latter was prepared as described in the literature.^[8] Although H₂Pc **2** shows less π - π stacking and a slightly better solubility in organic solvents than its phenanthroline-appended analogue,^[8] it was still not possible to perform purification by chromatographic techniques or by recrystallization. Thus, the crude product had to be purified by thoroughly washing it with various solvents of different polarity to afford the pure H₂Pc **2** in 67% yield. The purity was confirmed by elemental analysis, IR, mass spectrometry (MALDI), and ¹H NMR spectroscopy.

Following our aim to probe coordination reactions with H₂Pc **2** as a ligand system, we could not fail to notice that its still-limited solubility prevented any success in such experiments. Therefore and alternatively, in trying to test the direct cyclotetramerization of a metal complex of a dinitrile precursor, the Pd^{II} complex **3** with the phthalonitrile derivative **1** as a ligand, was prepared (Scheme 1). However, although the reaction conditions have been varied to a large extent with respect to different solvents, catalytic bases, and different metal-ion templates, no Pc product from the Pd^{II} complex **3** could be characterized so far.

Synthesis of Asymmetrical Octasubstituted H₂Pcs (5–9)

The interest in asymmetrically substituted Pcs (e.g. 3:1 Pcs, where three of the benzenoid rings are substituted with solubilizing groups and the fourth one with ligating groups) is primarily based on the gain of solubility of the Pcs and

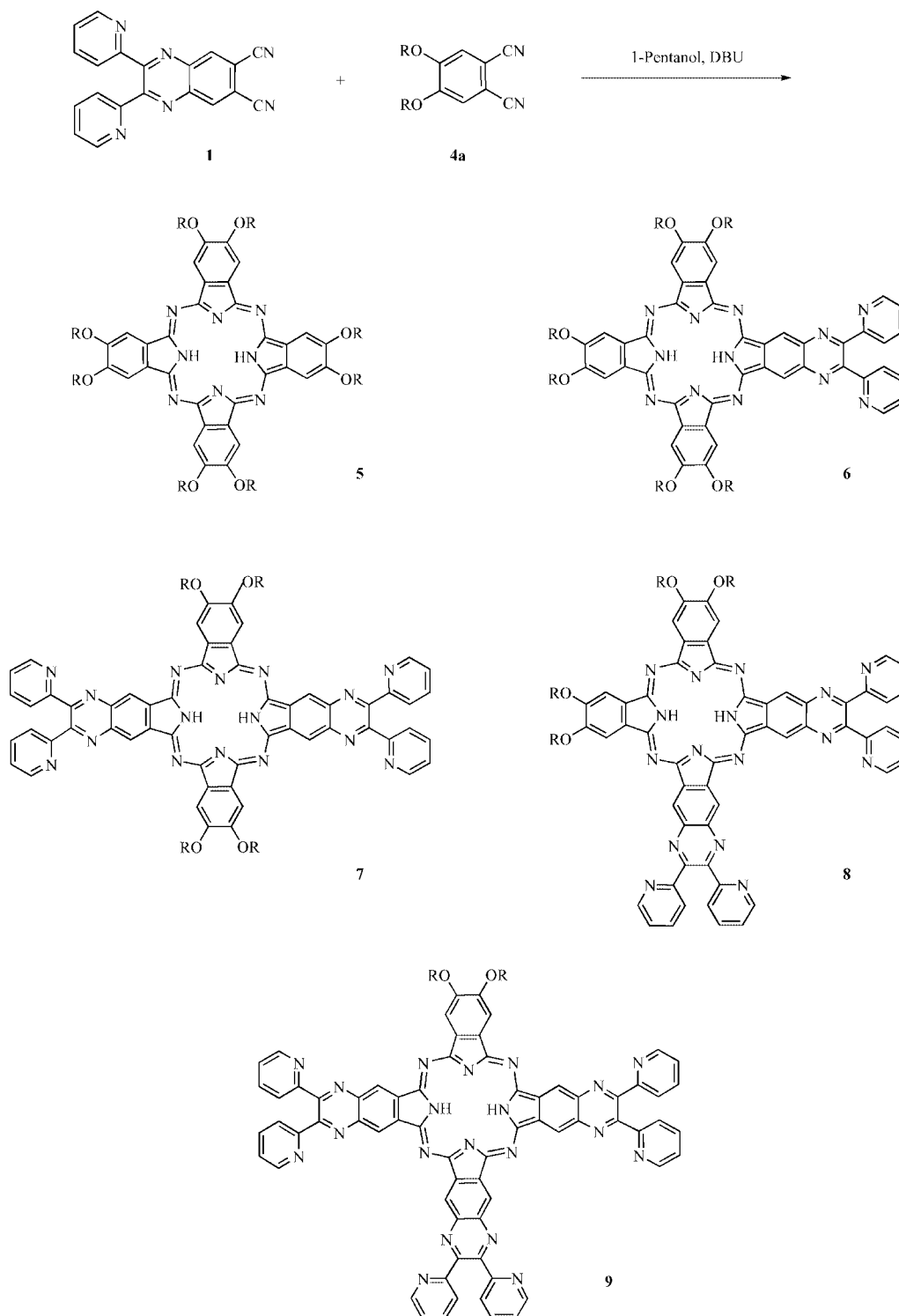


Scheme 1. Transformation of **1** into H₂Pc **2** and Pd(II) complex **3**.

the availability of peripheral coordination sites for binding metal ions. Additionally, the distinctly reduced aggregation of the Pcs' cores allows easier chromatographic separation of the different condensation products, and most importantly even for the two isomers.

There are reports in the literature^[11] describing the preparation of asymmetrically substituted 3:1 Pcs, in which the

most common strategy is a mixed cyclotetramerization reaction between two differently substituted phthalonitriles or diiminoisoindolines in a ratio, which is biased to give mostly the target 3:1 compound at the expense of other cross-condensation products. However, with this method, a mixture of products is inherently formed, which makes the separation and purification steps by means of chromato-



Scheme 2. Pcs **5–9** of the statistical condensation reaction of phthalonitriles **1** and **4a** ($R = p$ -pentylphenoxy).

graphic techniques quite difficult. Consequently, the isolation of all Pc products from a mixed cyclotetramerization reaction, including the different isomeric products, has rarely been reported.^[12]

For the present work, we selected two reactants for probing a statistical condensation reaction, namely the phthalonitrile derivative **1**, which is functionalized with two pyridyl groups, and 4,5-bis(*p*-pentylphenoxy)phthalonitrile **4a**. As expected, this procedure leads mainly to the formation of a mixture of H₂Pcs (**5–9**), as shown in Scheme 2 (the formation of H₂Pc **2** may also occur in a minor amount). Obviously, the central theme and challenge of such a strategy lies in the workup protocol for the mixed products. In the actual case, separation of the H₂Pcs **5** and **6** from the reaction mixture was successfully achieved by column chromatography. Pcs that have a larger number of the more polar pyridyl groups elute distinctly slower through the silica column. The remaining H₂Pc products **7–9** (except **2**) were isolated by preparative thin layer chromatography. Take, for example, the case of H₂Pc **8** with the four pyridyl groups located on adjacent benzo positions. We noticed that it is retained longer on alumina than its *trans* isomeric form, H₂Pc **7**. This illustrates what is still quite rare and, therefore, remarkable, namely the separation of isomeric Pcs by preparative thin layer chromatography on alumina. Finally, H₂Pcs **5–9** have been purified by refluxing in and washing with CH₃CN.

In general, by varying the molar ratio of the two different types of phthalonitrile precursors, it is, to some extent, possible to modify the relative amounts of the individual species which are present within the reaction mixture.^[11] In our study, we found that the 3:1 ratio of compounds **1** and **4a** optimizes the conditions for the formation of the asymmetrical H₂Pc **6**. The yields of H₂Pcs **5** and **6** are 26% and

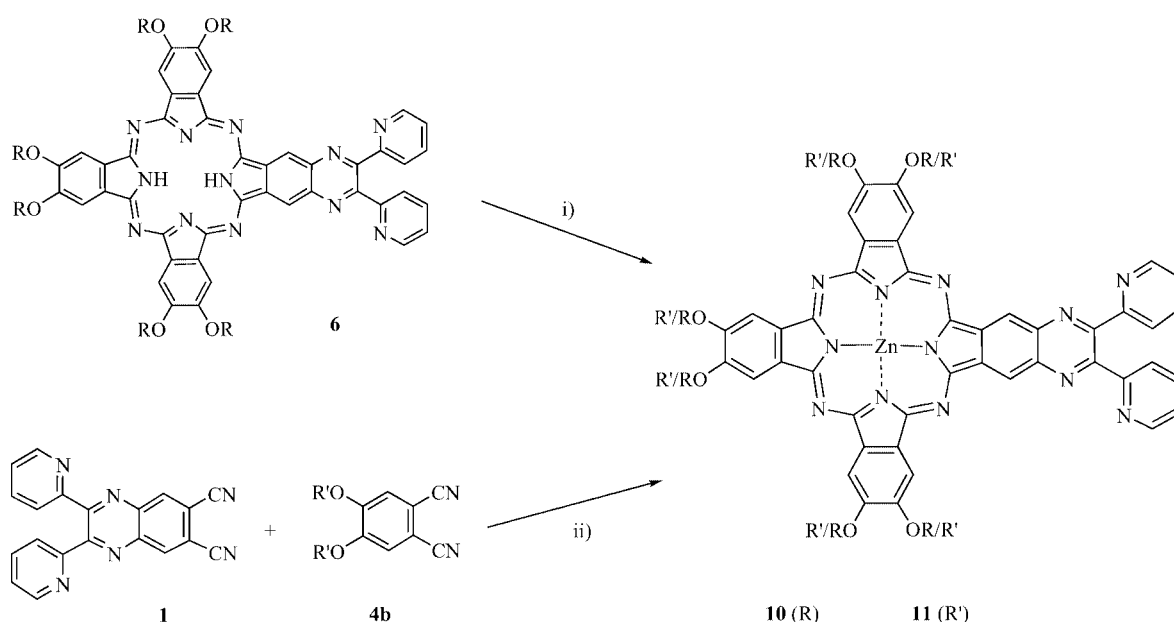
21%, respectively, which are quite comparable to values reported in the literature.^[11]

Synthesis of Asymmetrically Octasubstituted ZnPcs (**10**, **11**)

A reaction of H₂Pc **6** with Zn(II) acetate dihydrate in 1-pentanol under mild conditions gives ZnPc **10** in a fairly good yield (Scheme 3). The ZnPc **10** exhibits a solubility in common organic solvents that is conducive to an investigation by ¹H NMR and UV/Vis spectroscopy; however, the crystals obtained were of rather poor quality for a single-crystal X-ray study. Therefore, in order to elucidate the X-ray structure of such an asymmetrically octasubstituted system, the analogous 3:1 ZnPc **11** was prepared by the cyclotetramerization reaction of 4,5-bis[*p*-(*tert*-butyl)phenoxy]phthalonitrile^[13,14] **4b** and phthalonitrile derivative **1** with a Zn(II) template (Scheme 3). The exchange of the peripheral substituents, namely *p*-pentylphenoxy with *p*-(*tert*-butyl)phenoxy, was expected to give rise to a different crystallization behavior. Clearly, the reaction afforded a mixture of compounds from which, after several chromatographic purification steps, the 3:1 ZnPc **11** was isolated in 18% yield. Indeed, suitable single crystals for an X-ray analysis were obtained by slow evaporation from a pyridine solution.

X-ray Single-Crystal Structures

Crystal data for ligand **1**, its Pd^{II} complex **3**, and the ZnPc **11** are listed in Table 1. Compound **1**, the 2,3-di(2-pyridyl)-6,7-dicyanoquinoxaline ligand, crystallizes in the triclinic space group *P* $\bar{1}$ with one molecule per asymmetric unit. The molecular structure, together with selected bond



Scheme 3. Synthesis of ZnPcs **10** (*R* = *p*-pentylphenoxy) and **11** (*R'* = *p*-(*tert*-butyl)phenoxy). Reaction conditions: i) Zn(OAc)₂·2H₂O, 1-pentanol, 140 °C; ii) Zn(OAc)₂·2H₂O, 2-(dimethylamino)ethanol, 110 °C.

Table 1. Selected crystal data.

	1	3	11
Chemical formula	C ₂₀ H ₁₀ N ₆	C ₂₀ H ₁₀ Cl ₂ N ₆ Pd·C ₂ H ₃ N	C ₁₀₉ H ₉₉ N ₁₃ O ₆ Zn·7.5C ₅ H ₅ N
Molecular weight [g/mol]	334.34	552.69	2345.63
Crystal size [mm]	0.50 × 0.15 × 0.10	0.25 × 0.20 × 0.15	0.50 × 0.40 × 0.40
Crystal color	pale yellow	yellow	pink
Crystal shape	rod	block	block
Crystal system	triclinic	triclinic	monoclinic
Space group	<i>P</i> $\bar{1}$	<i>P</i> $\bar{1}$	<i>P</i> ₂ / <i>c</i>
<i>a</i> [Å]	7.582(1)	9.534(1)	27.097(1)
<i>b</i> [Å]	9.461(1)	9.902(1)	25.106(1)
<i>c</i> [Å]	12.205(2)	12.265(2)	19.666(1)
α [°]	102.74(2)	102.75(2)	90.00
β [°]	99.56(2)	97.34(1)	109.190(3)
γ [°]	104.69(2)	99.97(1)	90.00
Volume [Å ³]	802.8(2)	1095.6(2)	12635.3(9)
<i>Z</i>	2	2	4
Density (calculated) [g cm ⁻³]	1.383	1.675	1.233
μ [mm ⁻¹]	0.088	1.116	0.260
<i>F</i> (000)	344	548	4948
Index ranges <i>h</i>	−9 → 9	−10 → 10	−29 → 29
<i>k</i>	−11 → 11	−12 → 12	−28 → 29
<i>l</i>	−14 → 14	−15 → 15	−23 → 23
θ range for data collection [°]	2.49–26.00	2.16–26.01	1.14–25.00
Reflections: collected	6345	8532	97937
independent	2922	3964	20611
observed	1786	3196	12193
Parameters / restraints	235 / 0	289 / 0	1072 / 27
<i>R</i> indices <i>R</i> ₁	0.0737	0.0539	0.1140
(all data) <i>wR</i> ₂	0.0903	0.1089	0.2098
Final <i>R</i> indices <i>R</i> ₁	0.0392	0.0428	0.0753
[<i>I</i> > 2 σ (<i>I</i>)] <i>wR</i> ₂	0.0815	0.1048	0.1949
Goodness-of-fit on <i>F</i> ²	0.848	0.976	0.944
Min. ρ_e [e·Å ⁻³]	−0.162	−1.061	−0.725
Max. ρ_e [e·Å ⁻³]	0.207	1.008 near Pd1	0.959
Temperature [K]	153	153	153
Wavelength [Å] (Mo- <i>K</i> _α)	0.71073	0.71073	0.71073
Diffractometer used	Stoe IPDS I	Stoe IPDS I	Stoe IPDS II
Scan type	ϕ oscillation	ϕ oscillation	ω rotation
Solution	SHELXS-97	SHELXS-97	SHELXS-97
Refinement	SHELXL-97	SHELXL-97	SHELXL-97

lengths and bond angles, is shown in Figure 1. The structural parameters found for **1** are comparable to those found for other di(2-pyridyl)quinoxaline ligands.^[15] The benzene ring of the quinoxaline unit is nearly planar, whereas the pyrazine ring shows a slight distortion; the largest torsion angle is 6.8(3)° for N2–C3–C4–N1. Due to steric reasons, the pyridine rings are not coplanar to the quinoxaline system, and the torsion angles C3–C4–C5–N3 and C4–C3–C10–N4 are 35.6(3)° and 47.7(2)°, respectively. The pyridine N atoms are above and below the plane defined by the quinoxaline system, and the dihedral angle between the pyridine rings is 49.9(1)°. Figure 2 shows the crystal packing of compound **1**. C–H···N hydrogen bonds are present, resulting in the formation of dimers [C18–H···N6a 3.474(2) Å]. In addition, the molecules exhibit a head-to-tail arrangement, which is stabilized by π – π -stacking interactions with the shortest C···C contact being 3.379(2) Å.

Compound **3**, the Pd^{II} complex of ligand **1**, crystallizes in the triclinic space group *P* $\bar{1}$ with one complex molecule and one co-crystallized acetonitrile molecule per asymmetric unit. The molecular structure, together with selected

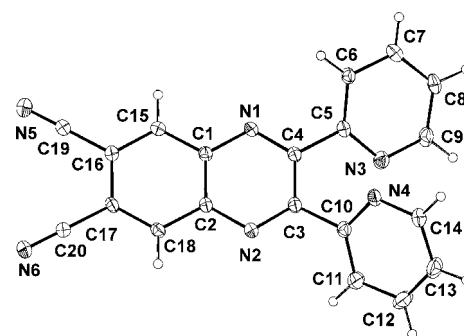


Figure 1. ORTEP representation (ellipsoids at 30% probability) of the molecular structure of **1**. Selected bond lengths and angles: C3–C10 1.491(2) Å, C4–C5 1.491(2) Å, C16–C19 1.442(3) Å, C19–N5 1.137(2) Å, C17–C20 1.447(2) Å, and C20–N6 1.148(2) Å; C3–C4–C5 121.42(15)°, C4–C3–C10 121.41(15)°, C16–C17–C20 119.19(15)°, and C17–C16–C19 119.75(15)°.

bond lengths and bond angles, is shown in Figure 3. The Pd^{II} ion is coordinated through both pyridine N atoms disposed in a *cis* conformation and through two terminal Cl

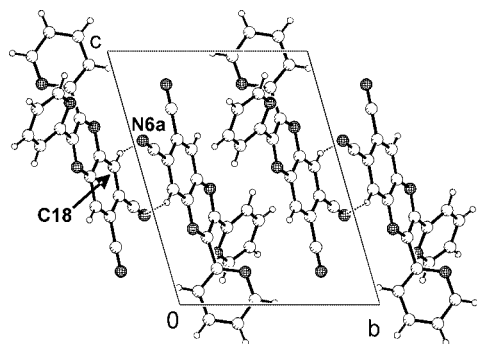


Figure 2. Crystal packing of **1** showing the formation of hydrogen-bonded dimers; C18-H...N6a 3.474(2) Å with symmetry operation $a: 2 - x, -y, 1 - z$.

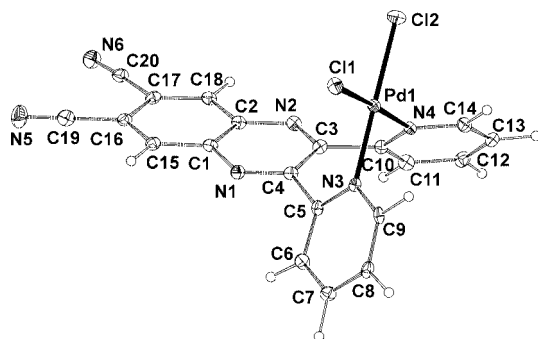


Figure 3. ORTEP representation (ellipsoids at 30% probability) of the molecular structure of **3**. The co-crystallized CH₃CN molecule has been omitted for clarity. Selected bond lengths and angles: Pd1–Cl1 2.2834(10) Å, Pd1–Cl2 2.2863(12) Å, Pd1–N3 2.010(4) Å, and Pd1–N4 2.028(3) Å; Cl1–Pd1–Cl2 93.92(4)°, Cl2–Pd1–N4 89.23(10)°, N4–Pd1–N3 86.95(13)°, and N3–Pd1–Cl1 89.95(9)°.

atoms. The metal ion adopts a square-planar coordination geometry with a deviation of 0.008(4) Å from the least-squares plane defined by the four donor atoms. Consequently, the pyrazine N atoms are non-coordinating, and ligand **1** adopts a seven-membered boat conformation, or equivalently, the pyridine rings are rotated with respect to the quinoxaline plane to show a butterfly wings arrangement.^[15] The torsion angles C4–C3–C10–N4 and C3–C4–C5–N3 are $-55.3(6)^\circ$ and $61.8(5)^\circ$, respectively, and the plane defined by the quinoxaline group is nearly perpendicular [$81.9(5)^\circ$] to that of the square-planar Pd^{II} coordination entity. Due to the coordination of both pyridine units, both pyridine N atoms are above the plane defined by the quinoxaline system, and dihedral angle between the pyridine rings is $87.0(2)^\circ$. The Pd–Cl and the Pd–N bond lengths are comparable to those of related compounds reported in the literature.^[15] Figure 4 shows the crystal pack-

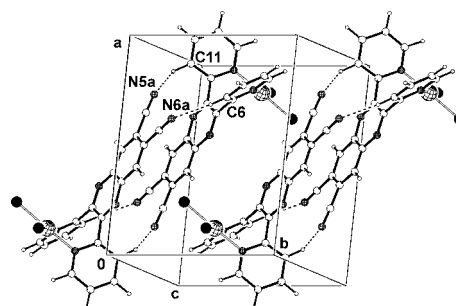


Figure 4. Crystal packing of complex **3** showing the formation of hydrogen-bonded/ π - π -stacked dimers; C6–H...N6a 3.368(6) Å and C11–H...N5a 3.543(7) Å with symmetry operation $a: -x, 1 - y, 1 - z$. CH₃CN molecules have been omitted for clarity.

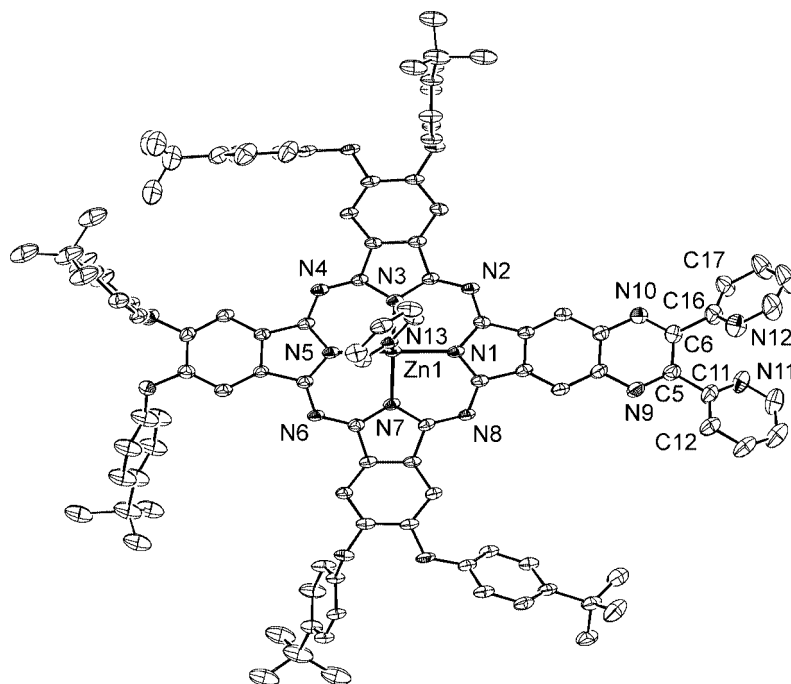


Figure 5. ORTEP representation (ellipsoids at 30% probability) of the molecular structure of **11** with an axial pyridine ligand. Hydrogen atoms have been omitted for clarity. Selected bond lengths and angles: Zn1–N1 2.240(3) Å, Zn1–N3 1.904(3) Å, Zn1–N5 2.197(3) Å, Zn1–N7 1.846(3) Å, and Zn1–N13 2.068(3) Å; N1–Zn1–N3 84.32(13)°, N3–Zn1–N5 89.84(13)°, N5–Zn1–N7 86.91(12)°, N7–Zn1–N1 90.64(13)°, and N1–Zn1–N13 105.38(12)°.

ing of complex **3**. The complexes exhibit a head-to-tail arrangement stabilized by π - π -stacking interactions and hydrogen bonds, which results in the formation of dimers [C6-H...N6a 3.368(6) Å and C11-H...N5a 3.543(7) Å; the shortest C...C contact in the π - π -stacking is 3.460(6) Å].

Compound **11** crystallizes in the monoclinic space group $P2_1/c$ with one ZnPc molecule axially ligated by a pyridine molecule, and an additional 7.5 co-crystallized pyridine molecules per asymmetric unit. Figure 5 shows the molecular structure of the ZnPc complex, together with selected bond lengths and bond angles. The Zn(II) ion is coordinated in a distorted square-pyramidal coordination geometry and situated out of the least-squares plane of the four coordinating Pc N atoms (N1, N3, N5, and N7) by 0.388(2) Å. The corresponding Zn–N bond lengths vary by 0.39 Å, which reflects the distortion of the coordination geometry around the Zn^{II} ion originating from the asymmetrical peripheral substitution of the Pc core. The bond length of the axially coordinated pyridine N to the Zn atom is 2.068(3) Å, which is similar to that of a previously reported structure.^[7f] The pyridine ring is slightly tilted from an orthogonal position with respect to the Pc plane with a dihedral angle of 81.0(1)°.

The aromatic Pc skeleton is distorted from perfect planarity by 0.063 Å from its best least-squares plane. The pyridine rings at the periphery of the Pc show the butterfly wings arrangement; the torsion angles C6–C5–C11–N11 and C5–C6–C16–N12 are –36.4(7)° and –49.1(7)°, respectively, with the N atoms above and below the Pc plane. Figure 6 shows the formation of hydrogen-bonded dimers. Two Pc complexes form a head-to-tail arrangement with respect to the quinoxaline unit. The interplanar distance between these two Pcs is 3.187(4) Å and the Zn...Zn distance is 5.458(5) Å. The Pc dimers are arranged in a zigzag pattern, exhibiting an angle of 57.50(1)°, as is shown in the crystal-packing diagram in Figure 7. A similar example of an asymmetric porphyrazine with bulky substituents that also forms analogous dimers in the solid state is reported in the literature.^[16]

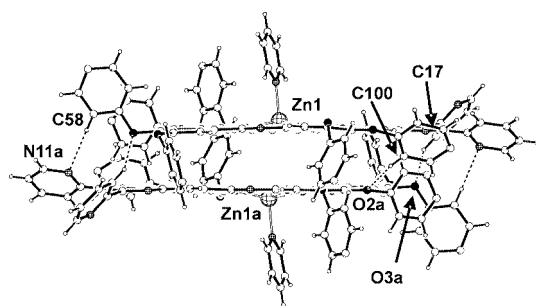


Figure 6. Hydrogen-bonded dimers of **11** with axial pyridine ligands. *tert*-Butyl groups have been omitted for clarity. Hydrogen-bond lengths: C17–H...O3a 3.135(6) Å, C58–H...N11a 3.536(8) Å, and C100–H...O2a 3.442(5) Å with symmetry operation $a: -1 - x, -y, -1 - z$.

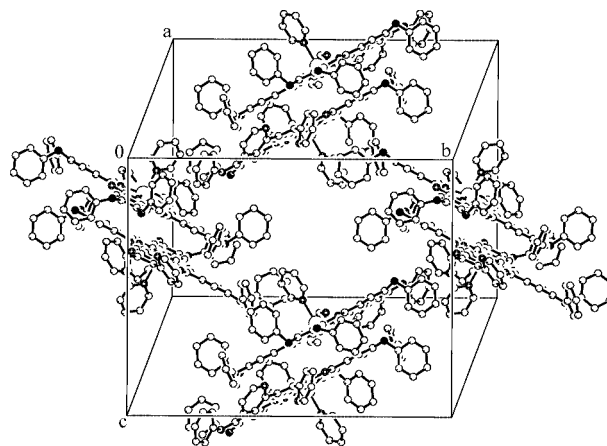


Figure 7. Crystal packing of compound **11** with an axial pyridine ligand. Hydrogen atoms and *tert*-butyl groups have been omitted for clarity.

Solution Properties of H₂Pcs 5–9

The presence of the *p*-pentylphenoxy groups in the H₂Pcs **5–9** leads to a fairly good solubility, which allows for ¹H NMR and UV/Vis spectroscopy in chloroform. From their ¹H NMR spectra, we can clearly show that all H₂Pcs **5–9** are well separated and isolated and represent pure compounds in accordance with their proposed molecular formula. Particularly, the ¹H NMR spectra are quite informative since they differentiate between the constitutional isomers **7** and **8**, which both show the same molecular ion peaks in their MALDI-MS spectra. As depicted in Figure 8, isomer **7** exhibits only two doublets, attributed to the two protons of the pyridyl groups (*ortho* to the N atom and *ortho* to the C linked to the quinoxaline unit), designated by c and d, respectively. Similarly, only one set of resonances is observed for the methylene protons of the pentylphenoxy chain closest to the Pc core (see the Experimental Section). Additionally, there are only two singlets assigned to the protons of the Pc core. Obviously, the spectrum of **7** indicates magnetically equivalent environments for these substituents, which conforms to a structure exhibiting, in good approximation, *D*_{2h} symmetry. Accordingly, in case of the less symmetrical isomer **8**, approximated by *C*_s symmetry, two types of methylene protons (see the Experimental Section) and two types of protons (c and d) of the pyridyl groups lead to separate triplets and doublets, respectively. Similarly, four types of Pc aromatic protons result in two separate singlets (a and b) in case of isomer **7**, whereas for isomer **8**, each one of them additionally splits into two separated singlets (a/a' and b/b').

The UV/Vis spectra within the Q band range of H₂Pcs **5–9**, in CHCl₃ solution, are shown in Figure 9. To recall, in general, the Q band of Pc is assigned as the transition from the HOMO to the LUMO, whereas for ring-expanded systems, the percentage of pure HOMO–LUMO character increases with enlargement of the π -system; with the same trend, due to the lowering of the LUMO, the Q band also shifts to longer wavelength. Furthermore, substituted species concomitantly split, which means that the degeneracy

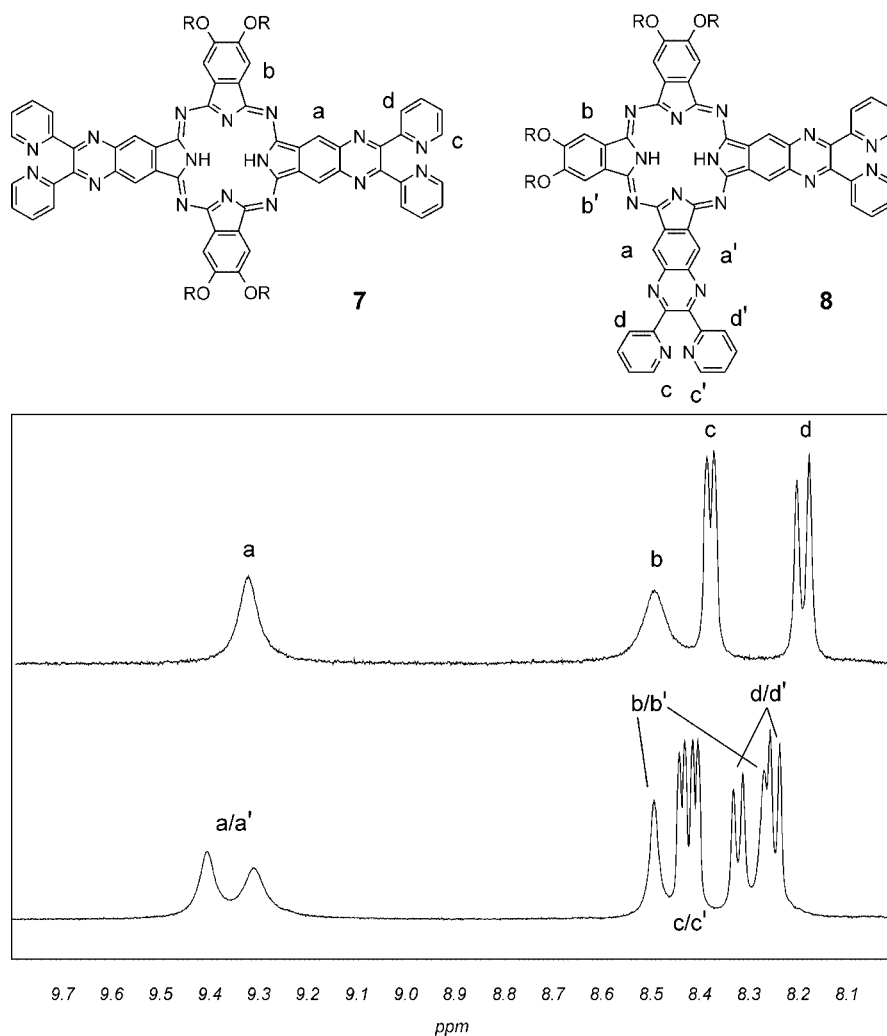


Figure 8. The ^1H NMR spectra (part of the resonance range of the aromatic protons) of H_2Pc compounds **7** (above) and **8** (below).

of the LUMO depends on the symmetry of the macrocyclic system, and this splitting becomes larger the larger the size

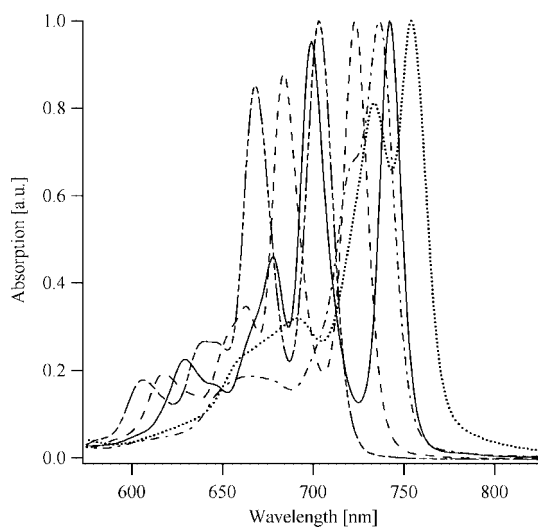


Figure 9. Q band range of UV/Vis spectra of H_2Pc compounds **5** (—), **6** (---), **7** (····), **8** (- · - · -), and **9** (— · —) in CHCl_3 .

of the fused aromatic molecules. As expected, compound **5**, the symmetrically substituted H_2Pc that shows approximately D_{2h} symmetry, exhibits a Q band with distinct splitting. In a recognizable manner, going from compounds **5** to **9**, the Q bands show a pronounced increase of their red shift and, from **5** to **7**, also an increase in their splitting. In contrast, compound **8** reveals only a small splitting. However, this observation is rationalized by MO calculations, which show that the Q band splitting of adjacent ring-expanded 2:2 Pcs is smaller, if occurring at all, than for the opposite ring-expanded 2:2 Pcs.^[17]

Conclusion and Outlook

Our present work describes mainly the synthetic access to asymmetrical octasubstituted Pcs with peripheral metal-binding sites. At the beginning, the symmetrical octasubstituted Pc **2** with peripheral metal-binding sites was obtained by a cyclotetramerization reaction of 2,3-di(2-pyridyl)-6,7-dicyanoquinoxaline. However, due to its insufficient solubility in organic solvents, it was quite impossible to investigate its coordination ability to different metal ions at the periph-

ery. Furthermore, a direct cyclotetramerization of a corresponding metal-diimine complex under a variety of conditions was shown to be problematic. Consequently, an alternative strategy involving the synthesis of asymmetrical octa-substituted Pcs has been adopted. As a result, Pcs **5–11**, containing combinations of 2,3-di(2-pyridyl)pyrazino and *p*-pentylphenoxy or *p*-(*tert*-butyl)phenoxy substituent groups, have been prepared by means of statistical condensation reactions between two different types of phthalonitriles, and most importantly, have successfully been isolated by chromatographic techniques. In practice, this protocol provides not only a versatile and convenient pathway to new Pc derivatives in reasonable yields and high purity but also paves the way for the incorporation of different transition-metal ions into the cavity and the periphery of the Pc core, respectively.

Within this context, we note that the construction of multicomponent systems such as molecular dyads, triads, and higher-ordered arrays has received considerable attention since such compounds are expected to exhibit fascinating properties and to play an important role in the development of devices at the molecular level.^[18] The investigation of the binding abilities of the promising Pcs **6–11** to appropriate transition-metal ions is in progress in our laboratory. Meanwhile, in order to probe the feasibility of the present concept for the introduction of a variety of metal ions at the periphery of Pc moieties, a rigid dipyrido[3,2-*d*:2',3'-*f*]-quinoxaline-fused ZnPc system has been synthesized, which in turn was successfully reacted with [Ru(bipy)₂Cl₂] \cdot 2H₂O to afford a dyad system. The extent of electronic communication between the individual components (ZnPc and Ru^{II} chromophore), for both the ground state and the excited state, is currently under investigation. The same holds for a study of the subsequent peripheral metallation of ZnPcs **10** and **11** by a variety of transition-metal ions.

Experimental Section

Measurements: Melting points were determined with a Büchi 510 apparatus and are uncorrected. ¹H and ¹³C NMR spectra were recorded with a Bruker AC 300, AC 400, or AC 500 spectrometer. Chemical shifts (δ) are reported in ppm and were calibrated against TMS as an internal standard, unless stated otherwise. CHN analyses were performed on a Carlo Erba EA 1110 CHNS apparatus. Thermal gravimetric analyses (TGA) were performed with a Mettler STARe system. Infrared spectra were recorded with a Perkin–Elmer Spectrum One FT-IR spectrometer. Mass Spectra were recorded with an AutoSpecQ spectrometer with EI and with an FTMS 4.7T BioAPEX II for the ESI and MALDI ionization methods. UV/Vis absorption spectra were recorded with a Perkin–Elmer Lambda 10 spectrometer.

Materials: 2,2'-Pyridil (Aldrich), 4,5-dichlorophthalonitrile (Aldrich), and 4-pentylphenol (Fluka) were used as supplied without further purification; 4,5-diaminophthalonitrile,^[8] dichloro-bis(dimethyl sulfoxide)palladium(II),^[19] and 4,5-bis[*p*-(*tert*-butyl)phenoxy]phthalonitrile^[14] (**4b**) were synthesized according to literature procedures. All solvents were of commercial quality and dried, where necessary, according to standard procedures. All reactions were carried out, unless otherwise mentioned, under normal labo-

ratory conditions in air. Silica gel 60 (40–63 μ m, Fluka) and neutral and basic aluminum oxide (CAMAG) and TLC plates (0.25 mm aluminum oxide with fluorescent indicator UV254, 0.20 mm silica gel with fluorescent indicator UV254, Macherey–Nagel) were used for chromatography.

6,7-Dicyano-2,3-di(2-pyridyl)quinoxaline (1): To a mixture of 2,2'-pyridil (1.00 g, 4.71 mmol) and 4,5-diaminophthalonitrile (689 mg, 4.36 mmol), ethanol (40 mL) and glacial acetic acid (6 mL) were added. The reaction mixture was stirred at 85 °C for 4 h, and then cooled to 0 °C. The precipitate was filtered and washed with plenty of ice-cold ethanol. The product was collected and dried at 50 °C to yield a brass crystalline solid (1.30 g, 89%). M.p. 243–244 °C. ¹H NMR (300 MHz, [D₆]DMSO): δ = 9.12 (s, 2 H), 8.31 (d, *J* = 4.4 Hz, 2 H), 8.07–7.98 (m, 4 H), 7.44–7.40 (m, 2 H) ppm. ¹³C NMR (75.5 MHz, [D₆]DMSO): δ = 114.06, 115.55, 124.04, 124.12, 137.10, 137.14, 141.03, 148.31, 155.59, 155.62 ppm. IR (KBr): $\tilde{\nu}$ = 3435, 3055, 2239 (–CN), 1586, 1569, 1475, 1397, 1347, 1078, 1002, 922, 898, 795, 759, 748, 536 cm^{–1}. MS (EI): *m/z* (%) = 333 (100) [M – H]⁺; elemental analysis calcd. (%) for C₂₀H₁₀N₆ (334.34) C 71.85, H 3.01, N 25.14; found C 71.77, H 2.97, N 25.29. Single crystals suitable for an X-ray diffraction measurement were obtained as pale yellow rods by slow evaporation from a DMSO solution.

2,3,9,10,16,17,23,24-Tetrakis[2,3-di(2'-pyridyl)pyrazino]phthalocyanine (2): Lithium metal (36 mg, 5.19 mmol) was dissolved in 1-pentanol (3 mL) at 80 °C under dry N₂. To this lithium pentoxide solution, **1** (100 mg, 0.30 mmol) was added, and the reaction mixture was heated at 100 °C for 17 h. On cooling, the dark blue-green solution was treated with glacial acetic acid (5 mL) and acetone (70 mL). The resultant precipitate was collected by centrifugation, washed thoroughly with water, methanol, THF, and Et₂O, and then dried at 50 °C to yield **2** as a dark blue-green powder (66 mg, 67%). M.p. > 250 °C. ¹H NMR: (500 MHz, D₂SO₄, TSPA as internal standard set to 0 ppm): δ = 10.87 (s, 8 H), 9.27 (d, *J* = 5.1 Hz, 8 H), 8.93–8.92 (m, 8 H), 8.57–8.54 (m, 8 H), 8.40 ppm (d, *J* = 6.2 Hz, 8 H) ppm. IR (KBr): $\tilde{\nu}$ = 3433, 1586, 1568, 1473, 1434, 1346, 1098, 1078, 1028, 999, 790, 743, 705 cm^{–1}. UV/Vis (pyridine): λ_{max} (log ϵ) = 377 (4.3), 765 nm (4.5 mol^{–1} dm³ cm^{–1}). MS (MALDI): *m/z* = 1339.40 [M + H]⁺; elemental analysis calcd. (%) for C₈₀H₄₂N₂₄ \cdot 3H₂O (1393.40) C 68.96, H 3.47, N 24.12; found C 68.67, H 3.19, N 23.82. TGA shows an overall weight loss of 3.2% (calcd. for three molecules of water: 3.9%).

Dichloro[6,7-dicyano-2,3-di(2-pyridyl)quinoxaline]palladium(II) (3): A mixture of *cis*-dichloro-bis(dimethyl sulfoxide)palladium(II) (201 mg, 0.60 mmol) and **1** (149 mg, 0.45 mmol) was refluxed for 2.5 h in THF (20 mL). The resulting yellow suspension was filtered hot, washed with THF, water, and Et₂O and dried at 50 °C to yield **3** as a pale yellow solid (207 mg, 90%). Suitable crystals for X-ray diffraction were obtained as yellow blocks by dissolving this compound in hot acetonitrile followed by slow evaporation of the solvent. M.p. > 250 °C. ¹H NMR (300 MHz, [D₆]DMSO): δ = 9.35 (s, 2 H), 9.09 (d, *J* = 5.5 Hz, 2 H), 8.27 (t, *J* = 7.7 Hz, 2 H), 7.95 (d, *J* = 7.7 Hz, 2 H), 7.87–7.82 (m, 2 H) ppm. IR (KBr): $\tilde{\nu}$ = 3438, 2241 (–CN), 1601, 1488, 1351, 1084, 1061, 774, 762, 539 cm^{–1}. MS (ESI, CH₃CN): *m/z* = 532.94 [M + Na]⁺, 1042.88 [2M + Na]⁺; elemental analysis calcd. (%) for C₂₀H₁₀Cl₂N₆Pd \cdot 0.8CH₃CN (544.50) C 47.65, H 2.30, N 17.49; found C 47.38, H 2.16, N 17.17. TGA shows an overall weight loss of 6.2% (calcd. for 0.8 molecules of acetonitrile: 6.0%).

4,5-Bis(*p*-pentylphenoxy)phthalonitrile (4a): To a suspension of 4,5-dichlorophthalonitrile (0.50 g, 2.54 mmol) and potassium carbonate (2.00 g) in DMSO (10 mL), 4-pentylphenol (2.6 mL,

15.2 mmol) was added. The mixture was heated to 85 °C under N₂ for 15 min, followed by the addition of another portion of potassium carbonate (2.00 g). The reaction mixture was stirred at 85 °C for an additional 3 h and then cooled to room temp. and poured into water (100 mL). The water phase was extracted with CH₂Cl₂ (3 × 50 mL). The combined organic phases were dried with Na₂SO₄. After removal of the solvent under reduced pressure, chromatography of the residue on a neutral alumina column with CH₂Cl₂ as eluent afforded **4a** as a turquoise viscous oil. This oily compound was dried under high vacuum, during which it solidified. M.p. 74–75 °C. ¹H NMR (300 MHz, CD₂Cl₂): δ = 7.18 (d, *J* = 8.6 Hz, 4 H), 7.08 (s, 2 H), 6.92 (d, *J* = 8.6 Hz, 4 H), 2.55 (t, *J* = 7.5 Hz, 4 H), 1.60–1.51 (m, 4 H), 1.31–1.22 (m, 8 H), 0.82 (t, *J* = 6.8 Hz, 6 H) ppm. ¹³C NMR (75.5 MHz, CDCl₃): δ = 13.98, 22.47, 31.10, 31.44, 35.26, 109.91, 115.13, 119.84, 121.37, 130.33, 140.87, 151.86, 152.24 ppm. IR (KBr): ν̄ = 3433, 2930, 2231 (–CN), 1587, 1501, 1292, 1223 cm^{–1}. MS (EI): *m/z* (%) = 452 (68) [M⁺]; elemental analysis calcd. (%) for C₃₀H₃₂N₂O₂ (452.59) C 79.61, H 7.13, N 6.19; found C 79.51, H 7.30, N 6.17.

H₂Pcs (5–9): To a mixture of **1** (123 mg, 0.37 mmol) and **4a** (500 mg, 1.1 mmol) in 1-pentanol (9 mL), DBU (156 μL, 1.0 mmol) was added. The reaction mixture was refluxed at 148 °C for 17 h under N₂ and then poured into CH₃CN (100 mL). The green precipitate was filtered, washed with CH₃CN, and dried at 50 °C. The product mixture was dissolved in a minimum of chloroform, and the solution was subjected to column chromatography (SiO₂), eluting with a gradient of 1–10% CH₃OH in CH₂Cl₂. The first fraction (eluent: CH₂Cl₂/CH₃OH, 100:1, *R_f* = 1.0) was collected. After removal of the solvent under reduced pressure, the green precipitate was refluxed in CH₃CN, filtered hot, washed with CH₃CN, and dried at 50 °C to afford **5**. The second fraction (eluent: CH₂Cl₂/CH₃OH, 90:1, *R_f* = 0.7) was collected and purified by the same procedure as for **5** to afford **6**. The third fraction was eluted with CH₂Cl₂/MeOH (10:1) as a mixture. After removal of the solvent, this mixture was initially applied to a basic alumina column eluting with chloroform to remove a trace amount of **6** and then separated on an alumina preparative TLC plate with chloroform. Pcs **7** (*R_f* = 0.8), **8** (*R_f* = 0.5), and **9** (*R_f* = 0.1) were extracted from the aluminum oxide with CHCl₃/MeOH (5:1); **9** was again subjected to an alumina preparative TLC plate (CHCl₃/MeOH, 400:1) and then extracted from the aluminum oxide. After separation, all of these compounds were further purified following the same procedure as described for **5**.

2,3,9,10,16,17,23,24-Octakis(*p*-pentylphenoxy)phthalocyanine (5): Grass-green powder; yield 131 mg (26%). ¹H NMR (400 MHz, CDCl₃): δ = 8.53 (s, 8 H), 7.15–7.10 (m, 32 H), 2.52 (t, *J* = 7.70 Hz, 16 H), 1.61–1.54 (m, 16 H), 1.34–1.27 (m, 32 H), 0.87 (t, *J* = 6.5 Hz, 24 H) ppm. IR (KBr): ν̄ = 3437, 2926, 1607, 1506, 1440, 1399, 1275, 1219, 1166, 1086, 1016, 878, 751 cm^{–1}. UV/Vis (CHCl₃): λ_{max} (log ε) = 291 (4.7), 347 (4.8), 606 (4.4), 640 (4.6), 668 (5.1), 703 nm (5.2 mol^{–1} dm³ cm^{–1}). MS (MALDI): *m/z* = 1812.00 [M + H]⁺; elemental analysis calcd. (%) for C₁₂₀H₁₃₀N₈O₈ (1812.37) C 79.53, H 7.23, N 6.18; found C 79.58, H 7.37, N 6.12.

23,24-Bis[2,3-di(2'-pyridyl)pyrazinol]-2,3,9,10,16,17-hexakis(*p*-pentylphenoxy)phthalocyanine (6): Green powder; yield 133 mg (21%). ¹H NMR (400 MHz, CDCl₃): δ = 9.34 (br. s, 2 H), 8.59 (br. s, 2 H), 8.47 (br. s, 2 H), 8.44 (s, 2 H), 8.41 (d, *J* = 4.52 Hz, 2 H), 8.25 (d, *J* = 7.80 Hz, 2 H), 7.85 (dt, *J* = 7.7 Hz, 1.7 Hz, 2 H), 7.31–7.25 (m, 14 H), 7.19–7.17 (m, 4 H), 7.10–7.02 (m, 8 H), 2.66 (t, *J* = 7.7 Hz, 4 H), 2.54 (t, *J* = 7.7 Hz, 8 H), 1.71–1.63 (m, 4 H), 1.63–1.53 (m, 8 H), 1.37–1.30 (m, 24 H), 0.91–0.85 (m, 18 H) ppm. IR (KBr): ν̄ = 3435, 2926, 1605, 1506, 1472, 1400, 1273, 1205, 1167,

1089, 1015, 880, 745 cm^{–1}. UV/Vis (CHCl₃): λ_{max} (log ε) = 348 (5.0), 618 (4.6), 663 (4.8), 684 (5.2), 723 nm (5.3 mol^{–1} dm³ cm^{–1}). MS (MALDI): *m/z* = 1693.86 [M + H]⁺; elemental analysis calcd. (%) for C₁₁₀H₁₀₈N₁₂O₆ (1694.11) C 77.99, H 6.43, N 9.92; found C 77.88, H 6.53, N 9.80.

9,10,23,24-Tetrakis[2,3-di(2'-pyridyl)pyrazinol]-2,3,16,17-tetrakis(*p*-pentylphenoxy)phthalocyanine (7): Green powder. ¹H NMR (300 MHz, CDCl₃): δ = 9.32 (br. s, 4 H), 8.49 (br. s, 4 H), 8.37 (d, *J* = 4.3 Hz, 4 H), 8.18 (d, *J* = 7.7 Hz, 4 H), 7.81 (dt, *J* = 7.7, 1.3 Hz, 4 H), 7.41–7.31 (m, 16 H), 7.28–7.24 (m, 4 H), 2.67 (t, *J* = 7.6 Hz, 8 H), 1.73–1.62 (m, 8 H), 1.37–1.33 (m, 16 H), 0.90 (t, *J* = 6.7 Hz, 12 H) ppm. IR (KBr): ν̄ = 3436, 2924, 1587, 1505, 1473, 1404, 1356, 1273, 1206, 1168, 1096, 1014, 998, 880, 744 cm^{–1}. UV/Vis (CHCl₃): λ_{max} (log ε) = 349 (4.9), 630 (4.4), 678 (4.7), 699 (5.0), 742 nm (5.0 mol^{–1} dm³ cm^{–1}). MS (MALDI): *m/z* = 1575.65 [M + H]⁺.

16,17,23,24-Tetrakis[2,3-di(2'-pyridyl)pyrazinol]-2,3,9,10-tetrakis(*p*-pentylphenoxy)phthalocyanine (8): Green powder. ¹H NMR (400 MHz, CDCl₃): δ = 9.40 (br. s, 2 H), 9.31 (br. s, 2 H), 8.49 (s, 2 H), 8.43 (d, *J* = 4.3 Hz, 2 H), 8.41 (d, *J* = 4.3 Hz, 2 H), 8.32 (d, *J* = 7.6 Hz, 2 H), 8.27 (s, 2 H), 8.24 (d, *J* = 7.8 Hz, 2 H), 7.84 (dt, *J* = 7.6 Hz, 1.2 Hz, 4 H), 7.30–7.25 (m, 4 H), 7.23–7.13 (m, 16 H), 2.66 (t, *J* = 7.83 Hz, 4 H), 2.57 (t, *J* = 7.83 Hz, 4 H), 1.69–1.56 (m, 8 H), 1.36–1.30 (m, 16 H), 0.91–0.86 (m, 12 H) ppm. IR (KBr): ν̄ = 3435, 2925, 1586, 1505, 1446, 1346, 1273, 1204, 1166, 1090, 1071, 1013, 880, 742 cm^{–1}. UV/Vis (CHCl₃): λ_{max} (log ε) = 352 (5.0), 665 (4.6), 736 nm (5.3 mol^{–1} dm³ cm^{–1}). MS (MALDI): *m/z* = 1575.65 [M + H]⁺.

2,3-Bis(*p*-pentylphenoxy)-9,10,16,17,23,24-hexakis[2,3-di(2'-pyridyl)pyrazinol]phthalocyanine (9): Green powder. ¹H NMR (400 MHz, CDCl₃): δ = 9.41 (br. s, 2 H), 9.02 (br. s, 2 H), 8.98 (br. s, 2 H), 8.40 (d, *J* = 4.0 Hz, 2 H), 8.36–8.26 (m, 8 H), 8.09–8.05 (m, 4 H), 7.82 (t, *J* = 7.2 Hz, 2 H), 7.75 (t, *J* = 7.3 Hz, H), 7.28–7.19 (m, 14 H), 2.68 (t, *J* = 7.4 Hz, 4 H), 1.70–1.63 (m, 4 H), 1.37–1.33 (m, 8 H), 0.90 (t, *J* = 6.4 Hz, 6 H) ppm. IR (KBr): ν̄ = 3436, 2926, 1729, 1631, 1587, 1505, 1469, 1346, 1273, 1204, 1097, 1071, 999, 891, 744 cm^{–1}. UV/Vis (CHCl₃): λ_{max} (log ε) = 352 (4.9), 691 (4.5), 734 (4.9), 753 nm (5.0 mol^{–1} dm³ cm^{–1}). MS (MALDI): *m/z* = 1457.56 [M + H]⁺.

{23,24-Bis[2,3-di(2'-pyridyl)pyrazinol]-2,3,9,10,16,17-hexakis(*p*-pentylphenoxy)phthalocyaninato}zinc(II) (10): A mixture of **6** (50 mg, 30 μmol) and Zn(II) acetate dihydrate (32 mg, 146 μmol) in 1-pentanol was heated at 140 °C under N₂ overnight. Upon the addition of CH₃CN (50 mL), a precipitate, formed from the dark reaction mixture, was filtered, washed with CH₃CN, and dried at 50 °C. The crude product was dissolved in a minimum of CHCl₃ and subjected to column chromatography (SiO₂), eluting with CH₂Cl₂/MeOH (10:1). After removal of the solvent by rotary evaporation, the solid was refluxed in CH₃CN (30 mL), filtered hot, and washed with boiling CH₃CN. The product was dried at 50 °C to yield a greenish blue solid (39 mg, 74% yield). ¹H NMR (400 MHz, CD₂Cl₂): δ = 9.36 (br. s, 2 H), 9.03 (s, 2 H), 8.92 (s, 2 H), 8.61 (br. s, 2 H), 7.30–7.06 (m, 28 H), 6.87 (br. s, 2 H), 6.51 (br. s, 2 H), 2.68–2.58 (m, 12 H), 1.67–1.58 (m, 12 H), 1.37–1.18 (m, 24 H), 0.90–0.86 (m, 12 H), 0.74 (t, *J* = 6.9 Hz, 6 H) ppm. IR (KBr): ν̄ = 3436, 2925, 1603, 1506, 1450, 1402, 1348, 1270, 1205, 1168, 1090, 1026, 887, 745 cm^{–1}. MS (MALDI): *m/z* = 1755.77 [M + H]⁺. UV/Vis (CHCl₃): λ_{max} (log ε) = 366 (5.0), 711 nm (5.2 mol^{–1} dm³ cm^{–1}); elemental analysis calcd. (%) for C₁₁₀H₁₀₆N₁₂O₆Zn·H₂O (1775.50) C 74.41, H 6.13, N 9.47, found C 74.14, H 6.07, N 9.30. TGA shows an overall weight loss of 0.4% (calcd. for one molecule of water: 1.0%).

{23,24-Bis[2,3-di(2'-pyridyl)pyrazino]-2,3,9,10,16,17-hexakis[*p*-(*tert*-butyl)phenoxy]phthalocyaninato}zinc(II) (11): A mixture of **1** (17 mg, 51 μ mol), **4b** (63 mg, 148 μ mol), and Zn(II) acetate dihydrate (15 mg, 68 μ mol) was heated in 2-(dimethylamino)ethanol at 110 °C under N₂ overnight. To the reaction mixture, water and methanol were added, and the resulting suspension was centrifuged. The blue solid was collected and dried at 50 °C. The crude product was dissolved in a minimum of CH₂Cl₂ and subjected to column chromatography (SiO₂), eluting with CH₂Cl₂/MeOH with a gradient of 0.25–1 % CH₃OH in CH₂Cl₂. The greenish blue fraction (eluent: CH₂Cl₂/CH₃OH, 100:1) was proven to be the specific ZnPc **11**. Solvent was removed by rotary evaporation, and the product was dried at 50 °C to afford **11** as a greenish blue solid (15 mg, 18 % yield). IR (KBr): $\tilde{\nu}$ = 3437, 2924, 1628, 1508, 1440, 1268, 1217, 1179, 1090, 1027, 890, 859 cm⁻¹. MS (MALDI): *m/z* = 1670.78 [M]⁺. UV/Vis (CH₂Cl₂): λ_{max} = 370, 646, 725 nm. Single crystals, suitable for an X-ray diffraction measurement, were obtained as pink blocks by slow evaporation from a pyridine solution.

X-ray Crystallography: Data for the crystals of compounds **1** and **3** were collected with a Stoe IPDS I instrument, and for compound **11**, with a Stoe IPDS II instrument, with Mo-K α graphite monochromatic radiation. The structures were solved by direct methods with the program SHELXS-97.^[20] The refinement with full-matrix least-squares techniques and all further calculations were carried out with SHELXL-97.^[21] All non-H atoms were refined with anisotropic displacement parameters. For **1** and **3**, the hydrogen atoms could be located from Fourier difference maps, while for **11**, the hydrogen atoms were included in calculated positions. Finally, all hydrogen atoms were treated as riding atoms with SHELXL default parameters. An empirical absorption correction was applied to **3**, with the DELREFABS routine in PLATON03 (T_{min} = 0.299, T_{max} = 0.739).^[22]

Compound **11** contains a high number of co-crystallized pyridine molecules. It was not possible to locate these molecules due to a strong disorder and/or partial occupation. Therefore, the SQUEEZE instruction in PLATON03 was used to calculate the potential solvent-accessible volume in the unit cell; 4736 Å³ were calculated containing about 1248 electrons. 30 pyridine molecules (30 \times 42 electrons) per unit cell were included in all further calculations. In addition, in the ZnPc complex, four *tert*-butyl groups of the Pc ligand are disordered over two positions and refined with occupancies of 0.5 for the participating methyl groups and with the thermal parameter constrained to be equal in each *tert*-butyl group. The details of crystal and experimental data are given in Table 1.

CCDC-615083 to -615085 contain the supplementary crystallographic data for this paper. These data can be obtained free of charge from The Cambridge Crystallographic Data centre via www.ccdc.cam.ac.uk/data_request/cif.

Acknowledgments

Financial support from the Swiss National Science Foundation (grant No. 200020–107589) is greatly appreciated. We also thank Fredy Nydegger (University of Fribourg) for mass spectra and Prof. Peter Bigler (University of Bern) for NMR spectra.

- [1] a) *The Porphyrin Handbook*, vols. 15–20 (Eds.: K. M. Kadish, K. M. Smith, R. Guilard), Academic Press, San Diego, California, **2003**; b) M. J. F. Calvete, D. Dini, S. R. Flom, M. Hanack, R. G. S. Pong, J. S. Shirk, *Eur. J. Org. Chem.* **2005**, 3499–3509; c) G. de la Torre, P. Vázquez, F. Agulló-López, T. Torres, *Chem. Rev.* **2004**, 104, 3723–3750; d) B. Donnio, D. Guillon,

- R. Deschenaux, D. W. Bruce, in: *Comprehensive Coordination Chemistry II*, vol. 7, 357–627 (vol. Eds.: M. Fujita, A. Powell, C. A. Creutz), Elsevier, London, **2004**.
- [2] N. B. McKeown, *Phthalocyanine Materials: Synthesis Structure and Function*, Cambridge University Press, Cambridge, **1998**.
- [3] R. Wang, R. Li, Y. Li, X. Zhang, P. Zhu, P.-C. Lo, D. K. P. Ng, N. Pan, C. Ma, N. Kobayashi, J. Jiang, *Chem. Eur. J.* **2006**, 12, 1475–1485.
- [4] C. Loosli, C. Jia, S.-X. Liu, M. Haas, M. Dias, E. Levillain, A. Neels, G. Labat, A. Hauser, S. Decurtins, *J. Org. Chem.* **2005**, 70, 4988–4992.
- [5] a) J. Sly, P. Kasák, E. Gomar-Nadal, C. Rovira, L. Górriz, P. Thordarson, D. B. Amabilino, A. E. Rowan, R. J. M. Nolte, *Chem. Commun.* **2005**, 1255–1257; b) M. V. Martínez-Díaz, M. S. Rodríguez-Morgade, M. C. Feiters, P. J. M. van Kan, R. J. M. Dolte, J. F. Stoddart, T. Torres, *Org. Lett.* **2000**, 2, 1057–1060.
- [6] B. Ballesteros, G. de la Torre, T. Torres, G. L. Hug, G. M. A. Rahman, D. M. Guldi, *Tetrahedron* **2006**, 62, 2097–2101.
- [7] a) M. Kimura, T. Hamakawa, K. Hanabusa, H. Shirai, N. Kobayashi, *Inorg. Chem.* **2001**, 40, 4775–4779; b) A. González-Cabello, P. Vázquez, T. Torres, D. M. Guldi, *J. Org. Chem.* **2003**, 68, 8635–8642; c) A. González, P. Vázquez, T. Torres, *Tetrahedron Lett.* **1999**, 40, 3263–3266; d) K.-W. Poon, Y. Yan, X.-Y. Li, D. K. P. Ng, *Organometallics* **1999**, 18, 3528–3533; e) S. M. Contakes, S. T. Beatty, K. K. Dailey, T. B. Rauchfuss, D. Fenske, *Organometallics* **2000**, 19, 4767–4774; f) S. Y. Al-Raqa, M. J. Cook, D. L. Hughes, *Chem. Commun.* **2003**, 62–63; g) M. P. Donzello, Z. Ou, F. Monacelli, G. Ricciardi, C. Rizzoli, C. Ercolani, K. M. Kadish, *Inorg. Chem.* **2004**, 43, 8626–8636; h) M. P. Donzello, Z. Ou, D. Dini, M. Meneghetti, C. Ercolani, K. M. Kadish, *Inorg. Chem.* **2004**, 43, 8637–8648.
- [8] J. Rusanova, M. Pilkington, S. Decurtins, *Chem. Commun.* **2002**, 2236–2237.
- [9] a) J. Granifo, M. E. Vargas, M. T. Garland, R. Baggio, *Inorg. Chim. Acta* **2000**, 305, 143–150; b) E. Rotondo, A. Rotondo, F. Nicolò, M. L. Di Pietro, M. A. Messina, M. Cusumano, *Eur. J. Inorg. Chem.* **2004**, 4710–4717; c) A. Escuer, S. B. Kumar, M. Font-Bardía, X. Solans, R. Vicente, *Inorg. Chim. Acta* **1999**, 286, 62–66; d) A. Escuer, T. Comas, J. Ribas, R. Vicente, *Inorg. Chim. Acta* **1989**, 162, 97–103.
- [10] a) M. Cusumano, M. L. Di Pietro, A. Giannetto, F. Nicolò, B. Nordén, P. Lincoln, *Inorg. Chem.* **2004**, 43, 2416–2421; b) J. Granifo, M. T. Garland, R. Baggio, *Inorg. Chim. Acta* **2003**, 348, 263–270; c) R. L. Williams, H. N. Toft, B. Winkel, K. J. Brewer, *Inorg. Chem.* **2003**, 42, 4394–4400; d) D. P. Rillema, K. B. Mack, *Inorg. Chem.* **1982**, 21, 3849–3854.
- [11] a) M. S. Rodríguez-Morgade, G. De la Torre, T. Torres, in: *The Porphyrin Handbook*, vol. 15 (Eds.: K. M. Kadish, K. M. Smith, R. Guilard), Academic Press, San Diego, California, **2003**, pp. 125–160; b) M. J. Cook, *Chem. Rec.* **2002**, 2, 225–236; c) G. De la Torre, T. Torres, *J. Porphyrins Phthalocyanines* **2002**, 6, 274–284.
- [12] a) G. J. Clarkson, N. B. McKeown, K. E. Treacher, *J. Chem. Soc., Perkin Trans. 1* **1995**, 1817–1823; b) R. Polley, T. G. Linsen, P. Stihler, M. Hanack, *J. Porphyrins Phthalocyanines* **1997**, 1, 169–179.
- [13] D. Wöhrle, M. Eskes, K. Shigehara, A. Yamada, *Synthesis* **1993**, 194–196.
- [14] S. E. Maree, T. Nyokong, *J. Porphyrins Phthalocyanines* **2001**, 5, 782–792.
- [15] a) F. Nicolò, M. Cusumano, M. L. Di Pietro, R. Scopelliti, G. Bruno, *Acta Crystallogr., Sect. C* **1998**, 54, 485–487; b) O.-S. Jung, S. H. Park, Y. J. Kim, Y.-A. Lee, H. G. Jang, U. Lee, *Inorg. Chim. Acta* **2001**, 312, 93–99; c) S. C. Rasmussen, M. M. Richter, E. Yi, H. Place, K. J. Brewer, *Inorg. Chem.* **1990**, 29, 3926–3932.
- [16] E. V. Kudrik, E. M. Bauer, C. Ercolani, A. Chiesi-Villa, C. Rizzoli, A. Gaberkorn, P. A. Stuzhin, *Mendeleev Commun.* **2001**, 11, 45–47.

- [17] N. Kobayashi, H. Konami, in: *Phthalocyanines: Properties and Applications*, vol. 4 (Eds.: C. C. Leznoff, A. B. P. Lever), VCH Publishers, New York, **1996**, pp. 343–404.
- [18] a) J. L. Sessler, V. L. Capuano, A. K. Burrell, *Inorg. Chim. Acta* **1993**, 204, 93–101; b) D. LeGourri rec, M. Anderson, J. Davidson, E. Mukhtar, L. Sun, L. Hammarstr m, *J. Phys. Chem. A* **1999**, 103, 557–559; c) J. M. Lintuluoto, V. V. Borovkov, Y. Inoue, *Tetrahedron Lett.* **2000**, 41, 4781–4786; d) A. Harriman, R. Ziessel, *Coord. Chem. Rev.* **1998**, 171, 331–339.
- [19] J. H. Price, A. N. Williamson, R. F. Schramm, B. B. Wayland, *Inorg. Chem.* **1972**, 11, 1280–1284.
- [20] G. M. Sheldrick, SHELXS-97 Program for the Solution of Crystal Structures, University of G ttingen, G ttingen (Germany), **1997**.
- [21] G. M. Sheldrick, SHELXL-97 Program for the Refinement of Crystal Structures, University of G ttingen, G ttingen (Germany), **1997**.
- [22] A. L. Spek, *J. Appl. Crystallogr.* **2003**, 36, 7–13.

Received: July 18, 2006

Published Online: October 10, 2006